Morphological Changes of Porphyrin Films on Graphite by Perchloric and Phosphoric Acid Electrolyte Solutions: an Electrochemical-AFM Study

Rossella Yivlialin *[,1]*, *Marta Penconi* [2], *Gianlorenzo Bussetti* [1,2], *Marco Finazzi* [1], *Lamberto Duò* [1] *and Alberto Bossi* [2]

[1] Department of Physics, Politecnico di Milano, p.za Leonardo da Vinci 32, I-20133 Milano, Italy
[2] Institute of Molecular Science and Technologies of the CNR (ISTM), PST via G. Fantoli 16/15, I-20138 Milano, Italy; and SmartMatLab Center, via C. Golgi 19, I-20133 Milano, Italy

E-mail: rossella.yivlialin@polimi.it

Abstract

Organic molecules have been proposed as promising candidates for electrode protection in acidic electrolyte solutions, but few results are available to confirm this hypothesis. The use of porphyrins as graphite surface protecting agents in sulphuric acid (H_2SO_4) is one of the newest. With the aim of unveiling the mechanism of such a protective effect, in this paper we test the stability of a H_2TPP thin film when immersed in perchloric and phosphoric acid electrolyte solutions. In particular, both perchloric and phosphoric acids are well-known to interact with porphyrins, but only the perchloric acid is reported to directly degrade and oxidase the molecules.

The protective role of porphyrins is tested in the potential range where the pristine graphite undergoes an oxidation process that erodes the surface and eventually exfoliate the stratified crystal. The electrochemical analysis is obtained in a three-electrode cell, while the surface morphology is monitored *ex-situ* and *in-situ* by atomic force microscopy. Electrospray mass

analysis is employed to investigate the surface chemical degradation of H_2TPP. We find that the organic film is not stable in perchloric acid solution. Conversely, in phosphoric acid, the porphyrin film holds on the graphite surface avoiding corrosion.

At least at such high anodic potentials, these results provide a rationale and evidence the limits offered by free-base porphyrins in graphite protection. The protective action is limited to specific electrolytes (like sulphuric and phosphoric acids) and appears that the protection mechanism resides in the stability of the central cavity of the porphyrin molecule towards strong oxidants.

1. Introduction

Graphite is a long-established electrode in batteries thanks to its good mechanical properties and chemical stability. [1-3] Nevertheless, the demand for improving next generation batteries in terms of cost reduction, stability, high performances, and life span remains very high. In this frame, organic molecules have been proposed as candidates to fabricate protective layers on the electrode surfaces. [4] Notably, organic molecules can be specifically designed and functionalized to optimize graphite protection in different electrodic solutions. Moreover, organic molecules can be deposited on a surface by exploiting different techniques, some of which are cheap and easy to implement in an industrial process (e.g. drop casting) or to integrate in a production chain involving high vacuum systems. [5] Nevertheless, only few results are available in this research topic: in particular, the existence of a class of molecules with a clear protective role has not yet been proven and researchers are still exploring a broad range of possible candidates. Among them, porphyrin and porphyrinoid compounds attracted the attention because the porphyrin/graphite interface shows interesting assembling, [6] optical, [7] electronic and [8] chemical [9] properties. Recently, the authors proved that metal-free tetra-phenyl porphyrin (H_2TPP, **Figure 1**) grows following a Stransky-Krastanov mode on graphite [10] and they succeeded in controlling both the regime and methods to grow 2-D or 3-D phases

as well as [11] in finding a protocol to remove the excess of porphyrin clusters (the 3-D phase). [12] The H_2TPP 2-D phase covers almost uniformly the graphite surface.

Despite the electrochemical properties of porphyrins have been widely investigated in solution, [13,14] their stability when deposited onto an electrode surface is still under debate. We recently showed that the H_2TPP 2-D phase acts as a protective film for a graphite electrode in a conventional three-electrode cell. [15] In the work, a highly oriented pyrolytic graphite (HOPG), with or without a protective porphyrin overlayer, was immersed in a sulphuric acid (H_2SO_4) solution, which is the typical electrolyte in lead-acid batteries. On pristine HOPG, H_2SO_4 intercalates between graphite planes and produces CO, CO_2 and O_2 gases during carbon oxidation, leading to the swelling of the basal plane of graphite (blistering), as reported in the literature. [16-19] The presence of porphyrins on the electrode surface inhibits this process. The protective role of H_2TPP is noticeable considering that sulphuric acid solutions can be used as "solvents" to dissolve free-base porphyrin aggregates. [20] The protective action on the graphite electrode is due to the 2-D wetting layer. [15] Perchloric acid (HClO₄, typically employed in the exfoliation of the graphite) as well as other oxidizing agents are usually reported to affect the conjugated structure of pyrrole rings or methin bridges of the H_2TPP molecule; [19, 21] Phosphoric acid, on the other hand, is able to corrode the pristine graphite basal plane (without showing a clear blistering) [22, 23] and it also behaves as a porphyrin "solvent" similar to H_2SO_4. [20,21] Comparing the behaviour of protected HOPG in these three mineral acids (H_2SO_4, HClO₄, H_3PO_4), where only the perchloric one should be able to destroy the porphyrin system, allows more insight into the chemistry of graphite protection in acid solutions. To this end, we test a thin (nominally 12 Å-thick) H_2TPP film on graphite immersed in an electrochemical cell containing a 2 M solution of either HClO₄ or H_3PO_4. The 12 Å-film shows a widespread porphyrin 2-D phase, covered by 3-D crystals. [15] We observe that the porphyrin film is not stable in a HClO₄ solution soon after a single electrochemical scan performed by cyclic-voltammetry (CV): some areas of the sample result exposed and blisters immediately appear on

3

the graphite surface. Conversely, the porphyrin 3-D phase is still recognizable on the sample surface after the immersion in the H_3PO_4 solution during the AFM measurements. In this case, the CV treatment precluded a direct "*in situ*" analysis of the porphyrin film due to the formation of tars caused by phosphates. [23] Nonetheless, a comparison of morphological images with electrospray mass analysis, employed to investigate the surface chemical degradation of H_2TPP (in the Supplementary Information), allows proving the stability of the porphyrin film in phosphoric electrolyte.

2. Experimental Section

z-grade HOPG (Optigraph) is mechanically exfoliated with adhesive tape. H_2TPP is grown by physical vapour deposition (PVD) from a Knudsen Cell (KC) fitted on a Kenosistec KE500 system. The KC is filled with 30 mg of H_2TPP powder purchased from Sigma-Aldrich. The powder is degassed in vacuum until the base pressure of the PVD chamber (1-2 $\times$ 10^{-6} mbar) is restored. The graphite substrate is kept at room temperature during the deposition. A quartz-microbalance, placed close to the sample, monitors the molecular flux, which is kept constant at 0.6 Å/s. Calibration of the film growth is described elsewhere. [15]

The $HClO_4$ and H_3PO_4 electrolyte solutions (2 M) are prepared and deaerated by bubbling argon for several hours prior the use. The electrolyte solution is placed in a three-electrode cell where the HOPG is the working electrode (WE), a Pt wire acts as counter electrode (CE) and a second Pt wire is used as a quasi-reference electrode (QRef). The WE can be easily implemented inside the three-electrode cell and placed in contact with the electrolyte solution without any contamination. [24] Being a single Pt wire, the QRef is not at thermodynamic equilibrium, which can in principle shifts the reference potential. [24] The authors tested the stability of the Pt-QRef within the experimental conditions (time, temperature, solvent, etc.) and found a fixed and stable shift of + 0.740 ± 0.010 V with respect to the normal hydrogen electrode. [19]

A single cyclic-voltammetry (CV; scan rate 25 mV/s) sweep is acquired on the samples. In CV, the WE electrochemical (EC) potential is ramped linearly in time and the current flowing

through the WE is accordingly measured. With a scan rate of 25 mV/s, a good compromise between charge transfer and mass transport is obtained, as reported in the literature. [16-19] When extracted from the electrochemical cell, the sample is dried accurately with a stream of pure nitrogen.

Electrochemical atomic force microscopy (EC-AFM) has already proved its potentialities and versatility when *in-situ* analysis of surface electrode is required. [25,26] In particular, EC-AFM is used in combination with HOPG electrodes [27,28] and/or with organic molecules at the liquid/solid interface. [29,30] In this study, a commercial 5500 Keysight system is used for the *ex-situ* and *in-situ* atomic force microscopy (AFM) measurements. The AFM images are acquired in non-contact mode, to preserve the quality of the organic film.

3. Results and discussion

After the deposition of a nominal 12 Å-thick film of H_2TPP on HOPG, the surface topography is characterized by 3-D structures with sharp edges on top of a 2-D porphyrin phase (see **Figure 2**a). [10] The thickness of the 3-D crystals is about 2 nm, as indicated in the figure. These structures are stable in air. The different adhesion forces characterizing the molecular assembling of either 3-D or 2-D phases are distinctively resolved by the AFM cantilever in tapping mode and the phase-contrast image (**Figure 2**b) allows to distinguish both of them. [31] The light blue areas are assigned to the 3-D phase, while the dark blue parts to the 2-D phase, in agreement with our previous results. [15]

Samples are then immersed in the EC cell and subjected to a single CV scan either in $HClO_4$ or in H_3PO_4 electrolytes (2 M concentration). Typical voltammograms are reported in **Figure 3**. Panel *a* shows the data acquired for the $HClO_4$ solution. The positive and negative features above 0.70 V, observed even on the pristine graphite, [17,19] are related to the anion intercalation process. [19] The ratio between the charge transfer during the cathodic (negative) and anodic (positive) currents is about 0.25, suggesting an irreversible electrochemical process caused by

solvated ClO_4^- intercalation (fully reversible processes require a charge ratio equal to 1 and a 0.59mV difference between forward and reverse peak potentials). [16-19]

The presence of H_2TPP molecules at the graphite-electrolyte interface is ensured by specific anodic peaks, appearing in the CV at potentials between 0.4 - 0.6 V. In particular, two peaks (labelled as I and II in the figure) appear at $E_{p,a,I} = 0.45$ V and $E_{p,a,II} = 0.55$ V, respectively. These are related to the two one-electron oxidation processes of the porphyrin macrocycle (usually called E^1_{ox} and E^2_{ox}, respectively and mostly correlated to the activity of the N atoms). [32-34] Their presence in the voltammogram confirms also the good conductivity of the molecular film.

Similar redox peaks are also observed during the CV sweep in phosphoric acid solution (Figure 3b). Here, the position of the peaks is different with respect to the previous case (i.e. $E_{p,a,I} = 0.40$ V and $E_{p,a,II} = 0.70$ V) [34, 35] and peak I is barely visible with respect to peak II. The weak intensity of the former could reasonably support the different ability of the H_3PO_4 acid to protonate H_2TPP molecules due to the more acidic environment (H_3PO_4 is potentially a triprotic acid, contrary to the monoprotic $HClO_4$). [34] When the EC potential is tuned to higher values (up to 1.6 V), the EC current enhancement is ascribable to the formation of an oxidized layer on the sample surface in phosphoric acid. This process [19,23] is completely irreversible, as proven by the fact that only positive features are detected by CV in the chosen EC potential range.

After a single CV cycle in $HClO_4$, the sample is extracted and dried accurately. The film morphology is then studied ex-situ by AFM. **Figure 4**a reports the morphology observed on the sample surface after the treatment in $HClO_4$ solution. Conversely to what previously observed in H_2SO_4, [15] $HClO_4$ dissolves and degrades both the molecular 2-D phase and the 3-D structures, resulting in the exposition of the HOPG electrode directly to the effect of the acid environment. It is not possible to find areas where the HOPG substrate appears unaffected by the anion intercalation. [15] Here, blisters, produced by gases developed during the

decomposition of the intercalated anions underneath the graphite surface, [16-19] are found randomly on the surface. This proves that ClO_4^- anions succeed in reaching the HOPG basal plane, passing through the damaged 2-D phase, in contrast to former observation in H_2SO_4 under comparable conditions. [15] We also observe some round-shaped masses that could be molecular re-crystallizations, consequent to the immersion of the initial 3-D porphyrin crystals in the liquid or degraded porphyrin residues. This hypothesis is supported by the phase-contrast image (Figure 4*b*) that enhances a clear difference between the masses (in blue) and the remaining bare graphite areas (in yellow). In order to investigate the processes by which porphyrins degrade, after the CV scan, the colourless $HClO_4$ electrolyte solution was analysed *via* direct infusion into a mass spectrometer with electrospray ionization (ESI, see Supporting Information). ESI spectra reveals the presence of several peaks, with masses between 300-520 Da, which may be ascribed and are compatible with chemical fragmentation of the H_2TPP scaffold due to oxidation/degradation processes (Figure SI3; a possible interpretation of the peaks is reported in table SI1); interestingly, the ESI analysis evidences the absence of any detectable trace of residual H_2TPP in solution.

The microscopic analysis is more complicated when a phosphoric acid solution is employed. In fact, after a single CV in H_3PO_4 solution, the *ex-situ* AFM measurement does not allow to clearly distinguish any porphyrin structures (see **Figure 5***a*). The topography reveals a densely-structured surface, with a high roughness ($R_q = 0.883$ nm), while the weak contrast in the phase signal (Figure 5*b*) cannot be unquestionably assigned either to the presence of porphyrin areas or to an oxidized layer, in analogy to previous studies on the pristine HOPG. [19,23] Considering that phosphoric acid should not affect the porphyrin macrocycle (other than promoting protonation at the N atoms similarly to a sulphuric acid electrolyte), [15] the high surface roughness points to consider the coexistence, on the sampled surface, of deposits of oxidized material and porphyrins; dubious is the dissolution of the molecular H_2TPP film. Thorough ESI–mass analyses were performed and the results (Figures SI4-SI6) indeed reinforce the

hypothesis described. In fact, ESI spectra of just the clean and fresh electrolyte solution evidence that phosphoric acid produces oligomers with m/z up to 600Da (SI4); similarly, no significant peaks appear analysing the ESI spectra of the electrolyte solution after a single CV scan, on bare HOPG (other than those due to phosphate oligomers). These findings would explain the formation of insoluble deposits on the electrode surface as observed by AFM. Analogously, ESI spectra of the electrolyte used to perform a CV scan on the HOPG electrode covered with the 12 Å-thick H_2TPP do not show any additional significant peak (implying absence of porphyrin degradations). Even if peaks near the background noise could be perceived, they are not as intense as those seen in figure SI3 (*i.e.* the one referring to the perchlorate solution). This would prove the chemical stability of porphyrins in the phosphoric electrolyte.

With these information, the evolution of the 12 Å-thick film of H_2TPP is tested when simply immersed in phosphoric acid (i.e. without any applied anodic potentials). We noted that the substrate steps (see Figure 5) are sharper, in strong contrast to what previously observed with pristine HOPG in H_3PO_4 electrolyte, where carbon dissolution of the basal plane is unquestionably detected. [23] This represents a congruent, yet indirect, evidence that the porphyrin layer acts as a partially protecting surface agent. In **Figure 6**, we report the *in-situ* AFM investigation of the sample surface as immersed in H_3PO_4, before the application of any EC potential. Some porphyrin structures are still recognizable in the topography (panel *a*), showing a thickness which is about 2/3 of the one measured in air and stable during the microscope acquisition time. [36] In agreement with the topography, the phase-contrast measurement (panel *b*) detects a different signal at correspondence with the 3-D structures (in blue), with respect to the substrate (in yellow). Noticing, from these results, we can confirm the similar behaviour of H_3PO_4 and H_2SO_4 as porphyrin-solvent. [15,20]

   4. Conclusion

We have further explored the protective "anti-aging" property of H_2TPP films in preserving graphite electrodes during a single and highly oxidative electrochemical process. A thin H_2TPP film deposited on graphite is immersed in an electrochemical cell containing either perchloric or phosphoric acid electrolyte solutions. $HClO_4$ shows comparable oxidative properties as the sulphuric acid on the pristine HOPG basal plane, being, at the same time, an oxidant able to degrade the tetrapyrrole macrocycle. H_3PO_4, instead, behaves as a porphyrin-solvent similar to sulphuric acid. An *ex-situ* AFM study shows different changes on the porphyrin film morphology induced by the above-mentioned electrolytes. Results suggest a crucial role of the porphyrin-electrolyte chemistry. In fact, the perchloric electrolyte damages the porphyrin 2-D phase (through molecular degradation as evidenced by the mass spectrometry studies) allowing blisters formation on graphite electrode. Conversely, the non-oxidizing H_3PO_4 electrolyte preserves the porphyrin 2-D phase, and its protective role. In this case polyphosphate deposits form on the surface burring both the HOPG and the porphyrin layer.

Supporting Information are available: mass spectra of the reference H_2TPP; analysis on the $HClO_4$ electrolyte solution after the CV scan on the $HOPG-H_2TPP$ system; analysis on the H_3PO_4 electrolyte solution, fresh, after the CV scan on the bare HOPG and on the HOPG-H_2TPP system.

References

[1]   C. E. Banks, R. G. Compton, New electrodes for old: from carbon nanotubes to edge pyrolytic graphite, Analyst. 131 (2006) 15-21.

[2]   L. L Zhang, X. S. Zhao, Carbon-based materials as supercapacitor electrodes, Chem. Soc. Rev. 38 (2009) 2520-31.

[3]   F. Jeschull, D. Brandell, K. Edström, M. J. Lacey, A stable graphite negative electrode for the lithium-sulfur battery, Chem. Comm. 51 (2015) 17100-3.

[4]   R. C Alkire, P. N. Bartlett, J. Lipkowski, in *Advances in Electrochemical Science and Engineering. Electrochemistry of Carbon Electrodes*, Vol. 16, Wiley, New York, 2015.

[5]   G. Bussetti, S. Trabattoni, S. Uttiya, A. Sassella, M. Riva, A. Picone, A. Brambilla, L. Duò, F. Ciccacci, M. Finazzi, Controlling drop-casting deposition of 2D Pt-octaethyl porphyrin layers on graphite, Synth. Met. 195 (2014) 201-207.

[6]   Z.-Q. Zou, L. Wei, F. Chen, Z. Liu, P. Thamyongkit, R. S. Loewe, J. S. Lindsey, U. Mohideen, D. F. Bocian, Solution STM images, of porphyrins on HOPG reveal thatsubtle differences in molecular structure dramatically alter packing geometry, J. Porph. Phyalocyan. 9 (2005) 387-392.

[7]   T. Sagara, M. Fukuda, N. Nakashima, Electroreflectance study of hemin adsorbated on a HOPG electrode: estimation of molecular orientation and analysis of nanofaradaic electroreflectance signal due to the stark effect, J. Phys. Chem. B 102 (1998) 521-527.

[8]   S. Kera, H. Yamane, H. Fukagawa, T. Hanatani, K. K. Okudaira, K. Seki, N. Ueno, Angle resolved UV photoelectron spectra of titanyl phtalocyanine monolayer film on graphite, J. Electr. Spectr. Rel. Phen. 156-158 (2007) 135-138.

[9]   O. Joe, N. Kazuhiko, A. Yuki, A. Makoto, S. Hirokazu, T. Arata, H. Toshiki, Face-on and columnar porphyrin assemblies at solid/liquid interface on HOPG, CSJ Chemistry Letters 38 (2009) 570-571.

[10]   G. Bussetti, M. Campione, M. Riva, A. Picone, L. Raimondo, L. Ferraro, C. Hogan, M. Palummo, A. Brambilla, M. Finazzi, L. Duò, A. Sassella, F. Ciccacci, Stable alignment of tautomers at room temperature in porphyrin 2D layers, Adv. Funct. Mater. 24 (2014) 958-963.

[11]   G. Bussetti, M. Campione, L. Ferraro, L. Raimondo, B. Bonanni, C. Goletti, M. Palummo, C. Hogan, L. Duò, M. Finazzi, A. Sassella, Probing two-dimensional vs three-dimensional molecular aggregation in metal-free tetraphenylporphyrin thin films by optical anisotropy, J. Phys. Chem. C 118 (2014)15649-15655.

[12]   G. Bussetti, M. Campione, L. Raimondo, R. Yivlialin, M. Finazzi, F. Ciccacci, A. Sassella, L. Duò, Unconventional post-deposition chemical treatment of ultra thin H_2TPP film grown on graphite, Crystal Res. Technol. 49 (2014) 581-586.

[13]   P. Worthington, P. Hambright, R. F. X. Williams, J. Reid, C. Burnham, A. Shamim, J. Turay, D. M. Bell, R. Kikland, R. G. Little, N. Datta-Gupta, U. Eisner, Reduction potentials of seventy-five free-base porphyrin molecules: reactivity correlations and the prediction of potentials, J. Inorg. Biochem. 12 (1980) 281-291.

[14]   H. N. Fonda, J. V. Gilbert, R. A. Cormier, J. R. Sprague, K. Kamioka, J. S. Connolly, Spectroscopic, photophysical, and redox properties of some meso-substituted free-base porphyrins, J. Phys. Chem. 97 (1993) 7024-7033.

[15]   R. Yivlialin, G. Bussetti, M. Penconi, A. Bossi, F. Ciccacci, M. Finazzi, L. Duò, Vacuum-deposited porphyrin protective films on graphite: electrochemical atomic force

microscopy investigation during anion intercalation, ACS Appl. Mater. Interfaces 9 (2017) 4100-4105.

[16]   C. A. Gross, J. C. Brumfield, E. A. Irene, R. W. Murray, Imaging the incipient electrochemical oxidation of highly oriented pyrolytic graphite, Anal. Chem. 65 (1993) 1378-1389.

[17]   D. Alliata, R. Kötz, O. Haas, In situ AFM study of interlayer spacing during anion intercalation into HOPG in aqueous electrolyte, Langmuir 15 (1999) 8483-8489.

[18]   D. Alliata, P. Häring, R. Haas, H. Siegenthaler, Anion intercalation into highly oriented pyrolytic graphite studied by electrochemical atomic force microscopy, Electrochem. Comm. 1 (1999) 5-9.

[19]   G. Bussetti, R. Yivlialin, D. Alliata, A. Li Bassi, C. Castiglioni, M. Tommasini, C. S. Casari, M. Passoni, P. Biagioni, F. Ciccacci, L. Duò, Disclosing the early stages of electrochemical anion intercalation in graphite by a combined atomic force microscopy/scanning tunneling microscopy approach, J. Phys. Chem. C 120 (2016) 6988-6093.

[20]   R. H. Felton, Primary Redox Reactions of Metalloporphyrins. The Porphyrins, Physical Chemistry, Part C, Vol. 5 (Ed: D. Dolphin), Academic Press, New York, 1978.

[21]   D. Maitra, J. Byun, P. R. Andreana, I. Abdulhamid, G. M. Saed, M. P. Diamond, S. Pennathur, H. M. Abu-Soud, Mechanism of hypochlorous acid mediated heme destruction and free iron release, Free Radic Biol Med. 51(2) (2011) 364–373.
T. P. Wijesekera, D. Dolphin, Methods in Porphryin Photosensitization, Springer, Berlin **1985**.

[22]   A. Guenbour, H. Iken, N. Kebkab, A. Bellaouchou, R. Boulif, A. Ben Bachir, Corrosion of graphite in industrial phosphoric acid, Appl. Surf. Sci. 252 (2006) 8710-8715.

[23]   R.Yivlialin, L. Brambilla, G. Bussetti, M. Tommasini, A. Li Bassi, C. S. Casari, M. Passoni, F. Ciccacci, L. Duò, C. Castiglioni, Evolution of the graphite surface in phosphoric acid: an AFM and Raman study, Beilstein J. Nanotechnol. 7 (2016) 1878-1884.

[24]   G. Inzelt, Pseudo-Reference Electrodes, Springer, Berlin, 2013.

[25]   A. Davoodi, J. Pan, C. Leygraf, S. Norgren, In situ investigation of localized corrosion of aluminum alloys in chloride solution using integrated EC-AFM/SECM techniques, Electrochem. Solid-State Lett. 8 (2005) B21-B24.

[26]   R. Vidu, F. T. Quinlan, P. Stroeve, Use of in situ electrochemical atomic force microscopy (EC-AFM) to monitor cathode surface reaction in organic electrolyte, Ind. Eng. Chem. Res. 41 (2002) 6546-6554.

[27]   R. Wen, M. Hong, H. R. Byon, In situ AFM imaging of $Li-O_2$ electrochemical reaction on Highliy Oriented Pyrolitic Graphite with ether-based electrolyte, J. Am. Chem. Soc. 135 (2013) 10870-10876.

[28]   F. P. Campana, R. Kötz, J. Vetter, P. Novák, H. Siegenthaler, In situ atomic force microscopy study of dimensional changes during Li^+ ion intercalation/de-intercalation in highly oriented pyrolitic graphite, Electrochem. Comm. 7 (2005) 107-112.

[29]   T. Kouzeki, S. Tatezono, H. Yanagi, Electrochromism of orientation-controlled naphthalocyanine thin films, J. Phys. Chem. 100 (1996) 20097-20102.

[30]   J. Izquiredo, C. Kranz, Electrochemical techniques for investigating redox active macromolecules, Eur. Pol. J. 83 (2016) 428-449.

[31]   J. Tamayo, R. Garcia, Deformation, contact time, and phase contrast in tapping mode scanning force microscopy, Langmuir 12 (1996) 4430-4435.

[32]   C. Paul-Roth, J. Rault-Berthelot, G. Simonneaux, C. Poriel, M. Abdalilah, J. Letessier, Electroactive films of poly(tetraphenylporphyrins) with reduced bandgap, J. Electroanal. Chem. 597 (2006) 19-27.

[33]   Y.-J. Tu, H. C. Cheng, I. Chao, C.-R. Cho, R.-J. Cheng, Y. O. Su, Intriguing electrochemical behaviour of free base porphyrins: effect of porphyrin-meso-phenyl interaction controlled by position of substituents on meso-phenyls, J. Phys. Chem. A 116 (2012) 1632-7.

[34]   C. Inisan, J.-Y. Saillard , R. Guilard, A. Tabard, Y. Le Mest, Electrooxidation of porphyrin free bases: fate of the π-cation radical, New J. Chem. 22 (1998) 823-830.

[35]   Y. Cui, L. Zeng, Y. Fang, J. Zhu, C. H. Devillers, D. Lucas, N. Desbois, C. P. Gros, K. M. Kadish, Tuning the electrochemistry of free-base porphyrins in acidic nonaqueous media: influence of solvent, supporting electrolyte, and ring substituents, Chem. Electro. Chem. 3 (2016) 228-241.

[36] When blisters are measured in-situ or in air, we do not observe significant changes (see Ref. 19). The measured thickness decrease of porphyrin structure, as reported in the text, can arise from a partial dissolution of these assemblies inside the acid electrolyte.

Figure 1. Free-base tetra-phenyl-porphyrin (H_2TPP). A meso phenyl substituted tetrapyrrolic macrocycle (carbon atoms: black spheres; hydrogen atoms: silver spheres; nitrogen atom: blues spheres).
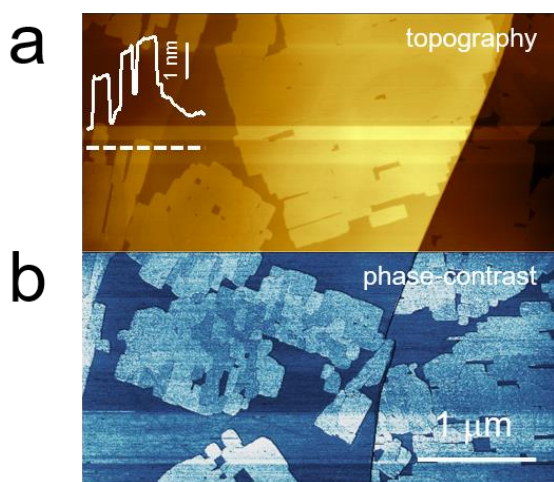

Figure 2. AFM non-contact image (4 x 4 μm^2) of the nominal 12 Å-thick porphyrin film before the electrochemical treatment. (**a**) Topography (4 x 2 μm^2). The profile scan (white line) of the 3-D structures is reported in the image. (**b**) Phase-contrast image (4 x 2 μm^2). We attribute the light blue areas to the 3-D phase, while the dark blue parts can be ascribed to the 2-D phase.
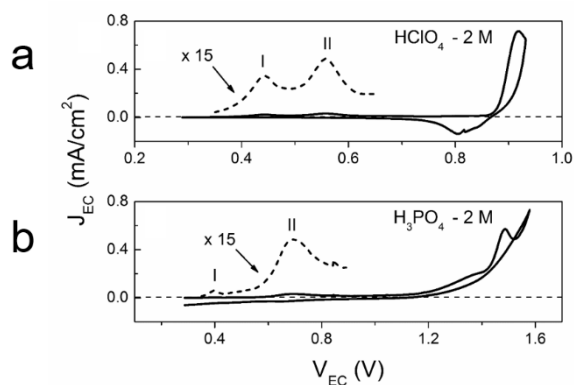
Figure 3. Cyclic-voltammetries acquired on the nominal 12 Å-thick porphyrin film with a scan rate of 25 mV/s. The faradaic current density (J_{EC}) is plotted as a function of the applied EC potential (V_{EC}) at the WE. (**a**) $HClO_4$ electrolyte. The two features (I and II) below 0.6 V are related to porphyrins, while the positive (anodic) current enhancement (above 0.85 V) indicates that the ClO_4^- anion intercalation occurs. The negative (cathodic) feature, centered at 0.80 V, suggests that graphite undergoes a partial de-intercalation process. (**b**) H_3PO_4 electrolyte. The two peaks (I and II) between 0.4 - 0.6 V are related to porphyrin electrochemical activity (dashed lines, currents are multiplied by a factor 15 for better clarity), while the anodic current enhancement (above 1.2 V) indicates processes at the graphite basal plane. The absence of any cathodic feature suggests that the chemical reaction is irreversible.
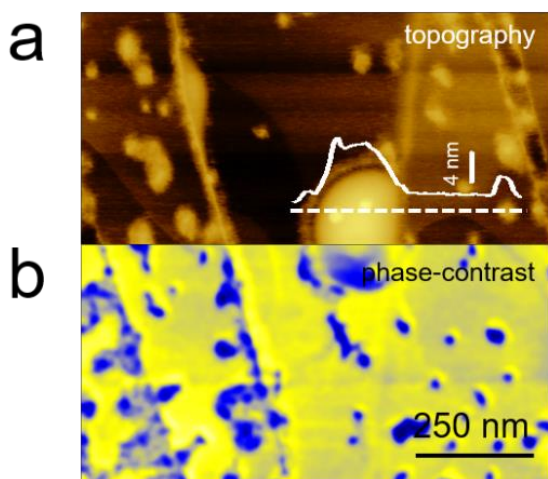

Figure 4. AFM non-contact image (4 x 4 μm^2) of the nominal 12 Å-thick porphyrin film after the treatment in a 2 M $HClO_4$ solution. (**a**) Topography (4 x 2 μm^2). The profile scan (white line) of the blister is reported in the image. (**b**) Phase-contrast image (4 x 2 μm^2). The porphyrin residual masses show a different signal (blue) with respect to the exposed graphite (yellow).
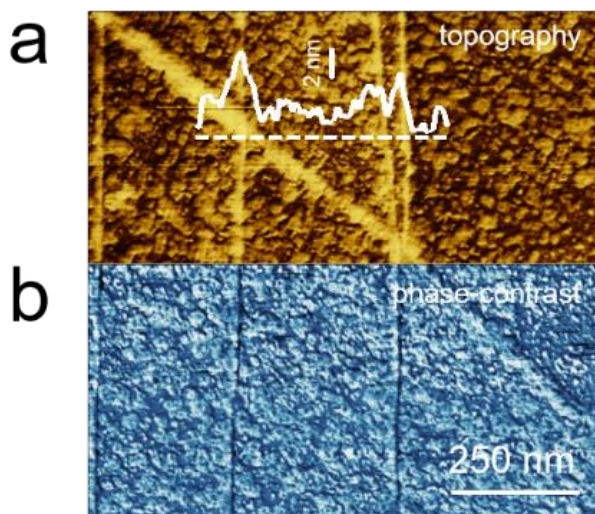
Figure 5. AFM non-contact image (4 x 4 μm^2) of the nominal 12 Å-thick porphyrin film after the treatment in a 2 M H_3PO_4 solution. (**a**) Topography (4 x 2 μm^2). The profile scan (white line) acquired across the graphite steps, is reported in the image. (**b**) Phase-contrast image (4 x 2 μm^2). The porphyrin residual masses uniformly cover the sample surface and an almost constant phase value is measured.
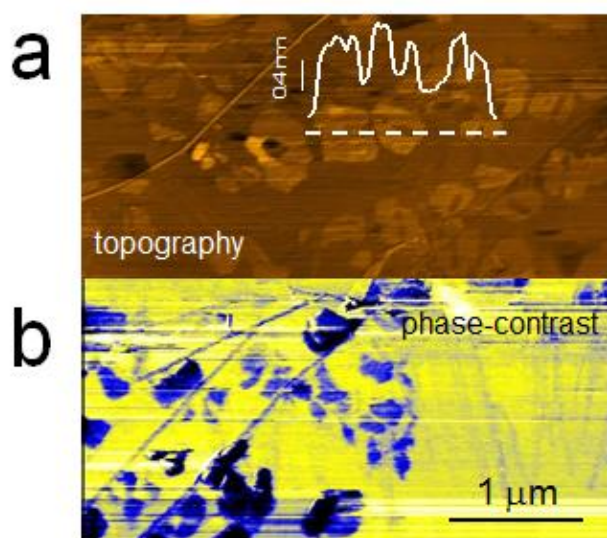

Figure 6. *In-situ* AFM non-contact image (4 x 4 μm^2) of the nominal 12 Å-thick porphyrin film in 2 M H_3PO_4 solution. (**a**) Topography (4 x 2 μm^2). The profile scan (white line) of the porphyrin crystals is reported in the image. (**b**) Phase-contrast image (4 x 2 μm^2). The porphyrin 3-D phase shows a different signal (blue) with respect to the 2-D phase (yellow).